

Comparative performance of focused and normal devices through a numerical study

Rambhatla G. Sastry and Kumar Praveer¹

Department of Earth Sciences, IIT, Roorkee – 247 667

¹BG Exploration & Production India Ltd., Ground Floor, MIDAS, Sahar Plaza, Kondivita
Andheri (E), Mumbai – 400 059

E-mail: rgsslfes@iitr.ernet.in / rgssastry@yahoo.com
Kumar.praveer@bg-group.com

ABSTRACT

The superiority of focussed devices over traditional Normal devices has remained a controversy in geophysical literature. A two-dimensional finite-difference scheme for numerical modeling of Normal and Laterlog (LL7) is undertaken to clarify the matters concerned. Spacing for spacing, normal log is better than LL7 for $e/AM > 1$ with $R_s = R_m$ and $R_t/R_m \leq 500$. Unlike the model tank experiment limitations (Roy & Appa Rao, 1976, 1978), in our numerical simulations, we could achieve perfect current focussing and evaluate the performance of existing alternate geometric factors due to Roy (1975) and Moran (1976). The computed R_a/R_m for LL7 was not even close to R_a/R_m under ideal conditions. But a simple two electrode device performs better in comparison to LL7 device provided $AM = A_1A_2$. This assertion is valid even for dynamic current ratio settings also.

INTRODUCTION

Laterolog (Doll 1951) was introduced for logging resistive thin beds, where unfocussed normal devices were supposed to fail. Doll (1953), Jiao & Sharma (1991) and Roy & Dutta (1997) have dealt the invaded zone to be a transitional zone. Many workers have studied and argued over the supremacy of laterolog devices over unfocussed ones (Doll 1951, 1953., Owen & Greer 1951; Guyod 1964; Roy & Dutta 1997; Roy & Apparao 1971, 1976, 1978; Roy 1975, 1976, 1977., Moran 1976; Jackson 1976, 1981; Repsold 1977; Moran & Chemali 1979., Hearst & Nelson 1985).

In view of inherent difficulties in physical modelling, Roy (1975) has suggested numerical modelling for a thorough analysis of the problem. Subsequently, several authors have attempted numerical modeling (Drahos 1984, Towle, Whitman & Kim, 1988; Roy & Dutta 1993, 1997; Pallavi 1996). However, the key question of laterolog performance vis – a – vis normal log in terms of better formation evaluation were not sufficiently addressed. In their finite-difference method (FDM) based simulation of LL7, Roy & Dutta (1997) even though adopted the concept of variable geometric factor did not short the guard or bucking electrodes, which violates the real practice. So, their claim that LL7 and Normal logs performance against a thin resistive bed are of similar

order of magnitude is untenable, for the basic principle of LL7 (Lynch 1962) is violated. Praveer (1997) has attempted an analysis of the problem in a better fashion and the present effort is an outcome of the same.

THEORETICAL FORMULATION

In an infinite homogeneous and isotropic borehole environment (Fig.1), the ideal laterolog 7 (LL7) measurement (Fig. 2a) ($A_1M_1M_1A_0M_2M_2A_2$) involves the focusing of current through central current electrode, A_0 and bucking current through auxiliary electrodes A_1 and A_2 . The potential, $V(0)$ at any one of the potential electrode pairs, (M_1',M_1) or (M_2',M_2) is measured; O_1 and O_2 are the mid points of the two pairs of potential electrodes (Fig.2a). The electrodes A_1 and A_2 are shorted and the current, I flowing through them is so adjusted that the potentials between the two pairs of potential electrodes is reduced to nil in an ideal situation (Lynch, 1962) or remain same (Roy & Dutta 1997). This ensures current focussing as a horizontal sheet (Fig. 2a) into the formation opposite to main power electrode, A_0 (Doll 1951, N.N 1958, 1969, 1972).

The fundamental relation governing the flow of steady d.c current in inhomogeneous earth medium in cylindrical coordinate system (Mufti 1980) is given by

$$\frac{\partial}{\partial r} \left[\sigma(r,z) \frac{\partial v(r,z)}{\partial r} \right] + \frac{\partial}{\partial z} \left[\sigma(r,z) \frac{\partial v(r,z)}{\partial z} \right] + \frac{1}{r} \left[\sigma(r,z) \frac{\partial v(r,z)}{\partial r} \right] + q(r,z) = 0 \quad (1)$$

Where

q , strength of current source (Am^{-3})
 σ , conductivity (S/m) and
 V , potential (Volts).

The differential equation (eqn.1) in association with appropriate boundary conditions are solved by finite difference method (Mufti 1980). The adopted finite-difference mesh (Figs 2b and 2c) and the details of FDM method as per flow-chart (Fig.3) are included in Annexure I. Successive over relaxation (SOR) method has been used as a solver. The resulting potential values when multiplied with suitable geometric factors yield apparent resistivity values.

Our 2D finite-difference software “ll7norm” based on the outlined theory has helped in designing several numerical experiments to test the supposed supremacy of LL7 device over normal device.

APPARENT RESISTIVITY COMPUTATIONS

Under the ideal homogeneous and isotropic conditions, for a constant current ratio, $I_0/I = 0.363$, the resistivity, $\bar{\rho}$ for a LL7 device (Roy 1975) is given by

$$\rho_{LL7} = \left(\frac{4\pi L}{\left\{ \frac{I}{0.7} + \frac{I_0}{0.2} + \frac{I}{0.3} \right\}} \right) V(0) \quad (2)$$

where

L , Distance between two auxiliary current electrodes ($= A_1A_2$),

I , Current through auxiliary electrodes

I_0 , Current passing through main central power electrode, A_0 .

For an inhomogeneous medium the apparent resistivity (Roy 1975) is given by

$$\rho_{LL7} = \left(\frac{4\pi L}{\left\{ \frac{\bar{I}}{0.7} + \frac{I_0}{0.2} + \frac{\bar{I}}{0.3} \right\}} \right) V(0) \quad (3)$$

Here the current through central power electrode, I_0 is maintained at a constant value and $\bar{I} = (\bar{I}_1 + \bar{I}_2)/2$, \bar{I}_1 and \bar{I}_2 are the currents through A_1 and A_2 respectively against an inhomogeneous medium. Specifically for an inhomogeneous medium, eqn (3) can be written as

$$\rho_{LL7} = \left(\frac{4\pi L}{\left\{ \frac{\bar{I}}{0.7} + \frac{1}{0.2} + \frac{\bar{I}}{0.3} \right\}} \right) \frac{V(0)}{\bar{I}} = \left(\frac{4\pi L}{\left\{ \frac{\beta}{0.7} + \frac{1}{0.2} + \frac{\beta}{0.3} \right\}} \right) \frac{V(0)}{\bar{I}} \quad (4)$$

In a homogeneous medium, $L = 2.032$ m and $\beta = \frac{\bar{I}}{I_0} = 2.736$ and $V(0)$ is the potential at null point O_1 or O_2 .

Then, apparent resistivity (Moran 1976) is given by

$$\rho_{LL7} = 1.41 \left(\frac{V(0)}{I_0} \right) \quad (5)$$

Apparent resistivity in case of Normal device ($AM=A_1A_2$) is given by

$$\rho_a = 4\pi \left(\frac{AM}{I_A} \right) \quad (6)$$

SOFTWARE VALIDATION

As is customary for any generated software, validation against standard results constitutes a crucial and an important step. Accordingly, the present software is also validated against three standard departure curve sets for Normal device (Lynch 1962; N.N, 1958, 1969, 1972).

Case I : Uninvaded, homogeneous and isotropic bed of infinite thickness:

Five different ratios of R_t/R_m were chosen and corresponding R_a/R_m were computed for four different values of AM/d . The results are included in Table 1 and are also displayed in Fig. 4a. Notice in each case that computed R_a/R_m values are close to R_t/R_m .

Table 1. Computed and actual departure curves (R_a/R_m values for different R_t/R_m and AM/d) for Normal device against a homogeneous, infinite medium

R_t/R_m	R_a/R_m					
	AM/d = 1.5		AM/d = 2.0		AM/d = 4.0	
	Actual	Com-puted	Actual	Com-puted	Actual	Com-puted
10	10.83	10.63	11.67	10.69	12.5	9.79
20	19.0	20.43	21.67	21.00	26.67	19.54
30	26.67	30.20	32.5	31.57	41.0	29.96
40	32.5	39.82	40.0	41.21	50.0	40.92
50	40.0	49.26	50.0	52.82	70.0	52.31

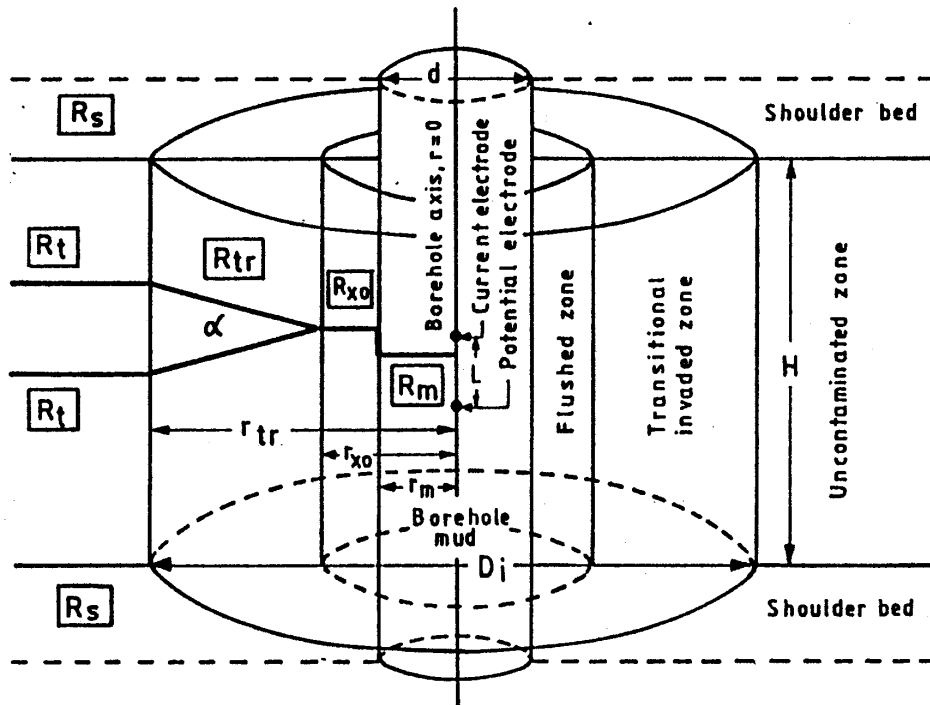


Figure 1. Borehole dc resistivity model exhibiting cylindrical symmetry around borehole axis with typical borehole environment (borehole mud of radius r_m with mud resistivity, R_m ; flushed zone of radius, r_{xo} with resistivity R_{xo} ; Invaded (transition) zone of radius r_{tr} (diameter of invasion, D_i) with resistivity R_{tr} ; Uninvaded or uncontaminated zone of thickness H and resistivity R_t ; Shoulder bed of resistivity, R_s lying above and below the bed under investigation) and position of current and potential electrodes of Laterolog 7 (LL7) setup C.E, Current electrodes and P.E, Potential electrodes (Roy & Dutta 1997).

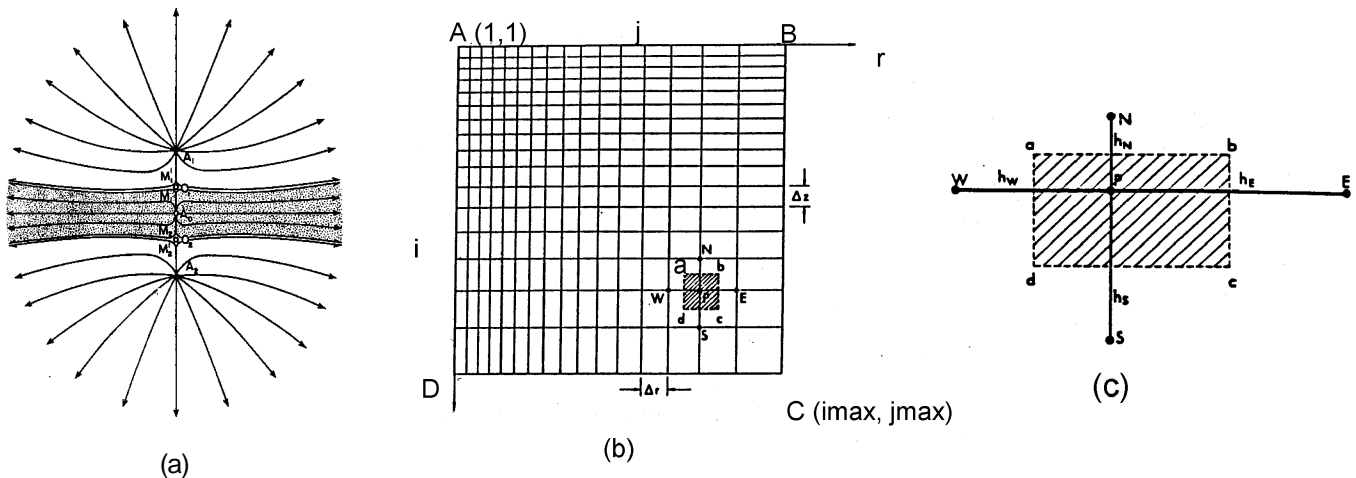


Figure 2. a) Schematic current flow pattern in a thin resistive bed using Laterolog 7 (LL7) device. A_0 , Main power electrode; A_1 and A_2 , auxiliary (bucking) power electrodes; M_1M_1' and M_2M_2' are potential electrode pairs; O_1 and O_2 are reference points for potential measurement. b) A typical finite difference mesh (FDM) for discretization of inhomogeneous earth medium surrounding the borehole. c) Rectangular FDM mesh element $abcd$ (Ref. Fig. 2b) showing grid spacings h_N, h_E, h_S and h_W in north, east, south and west directions with respect to node center, P .

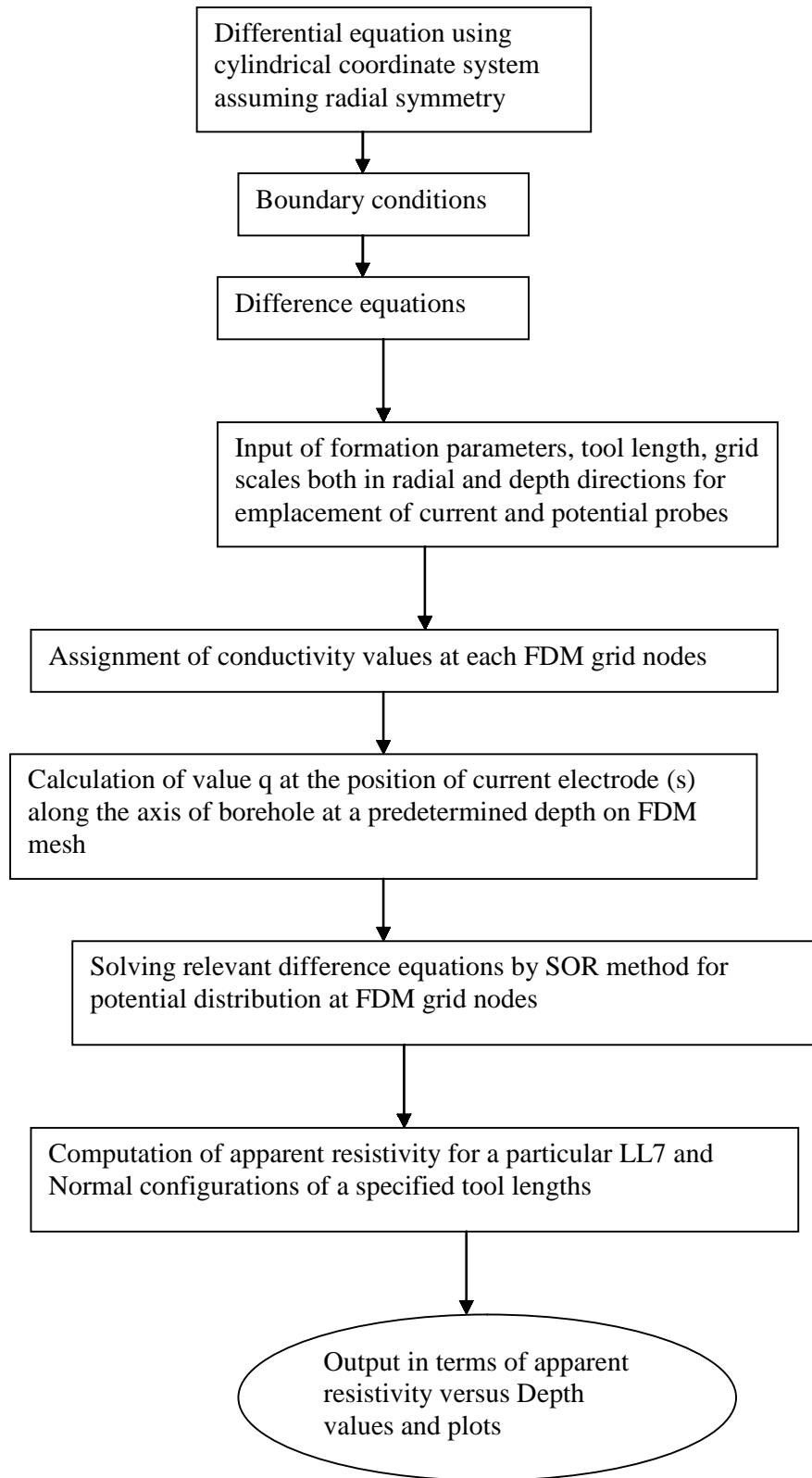


Figure 3. Flowchart of FDM based focussed log simulation algorithm

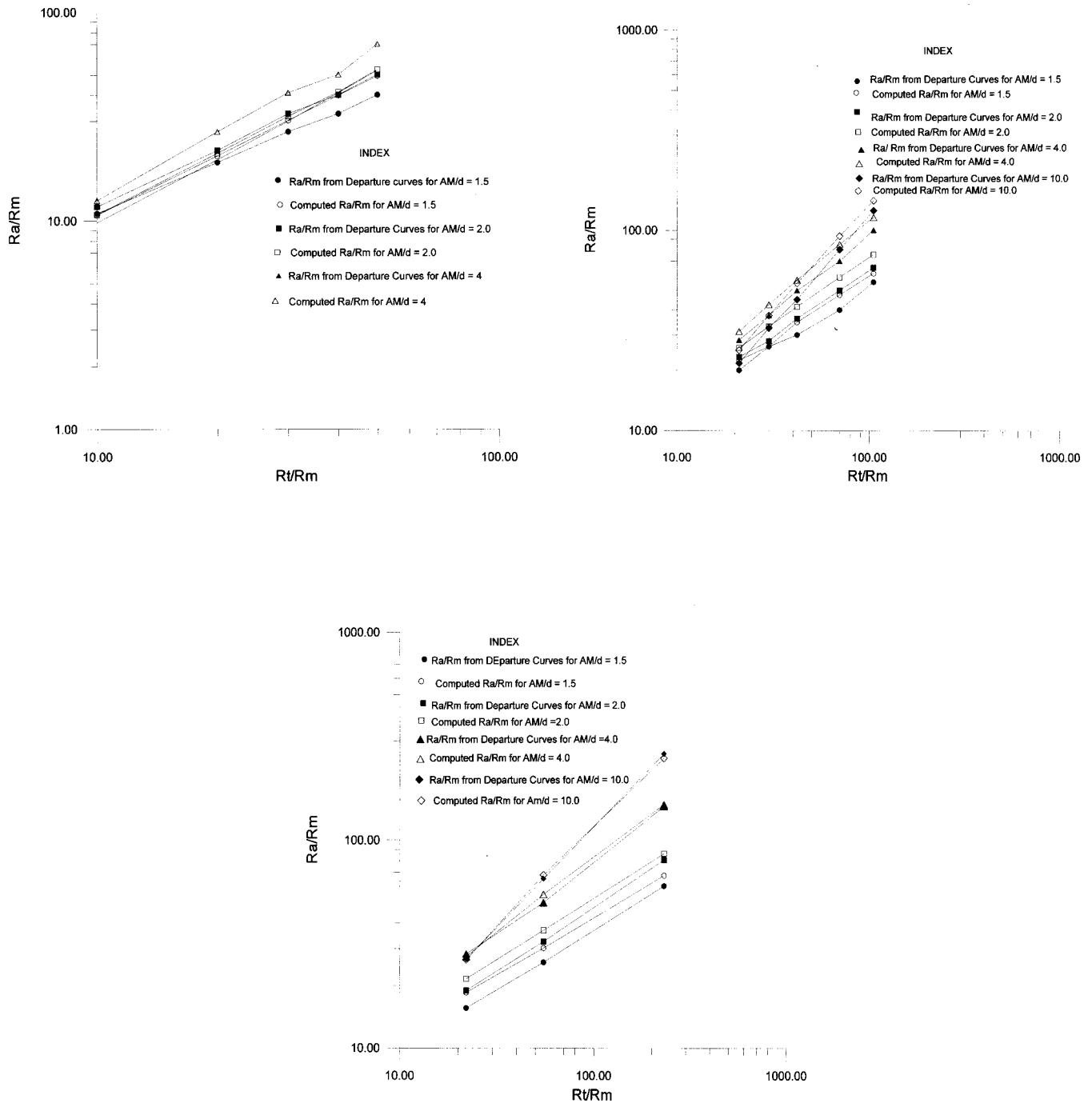


Figure 4. a) A portion of standard departure curves against an infinitely thick bed with no invasion condition for Normal device (Lynch 1962) is compared with the computed ones (Ref. Table 1). b) A portion of standard departure curves for Normal device against an invaded finite ($R_i/R_m = 21$; $D_i/d = 2$, $e/d = 50$) thick bed (Lynch 1962) is compared with computed ones (Ref. Table 2). c) A portion of standard departure curves for Normal device (Lynch 1962) against an invaded infinitely thick bed ($R_i/R_m = 11$; $D_i = 5d$) is compared with computed ones (Ref. Table 3).

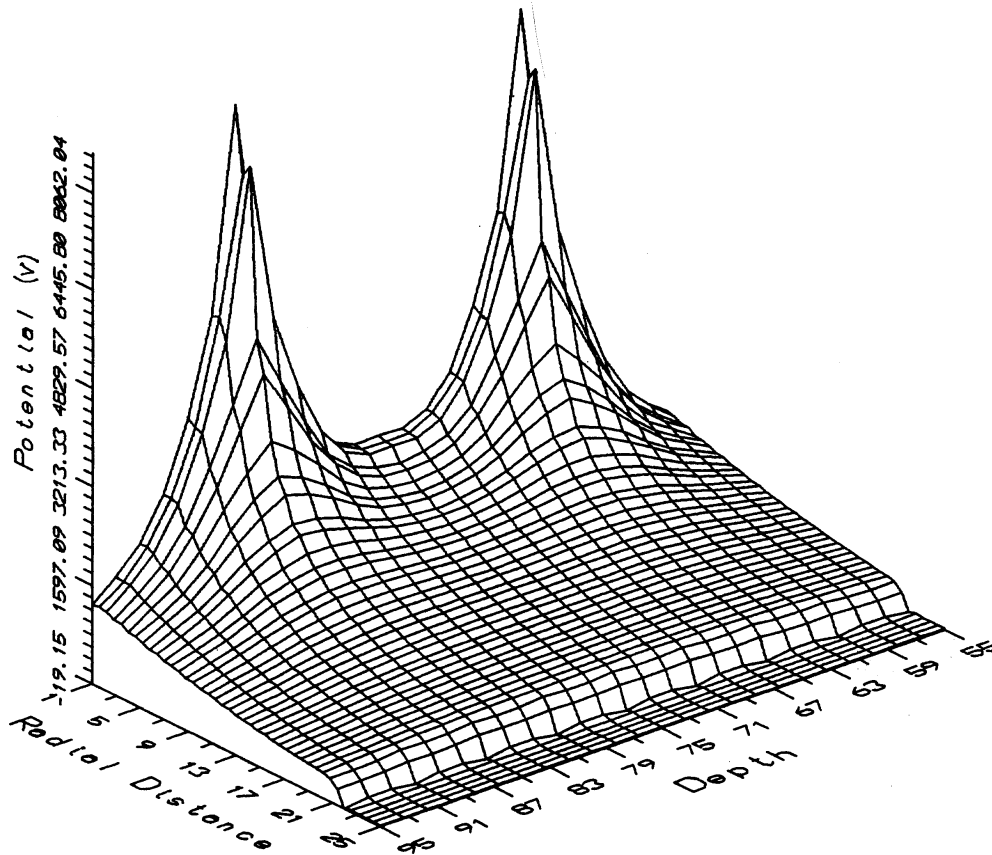


Figure 5. a) Potential surface plot with $O_1O_2 = 16''$ and $A_1A_2 = 80''$.

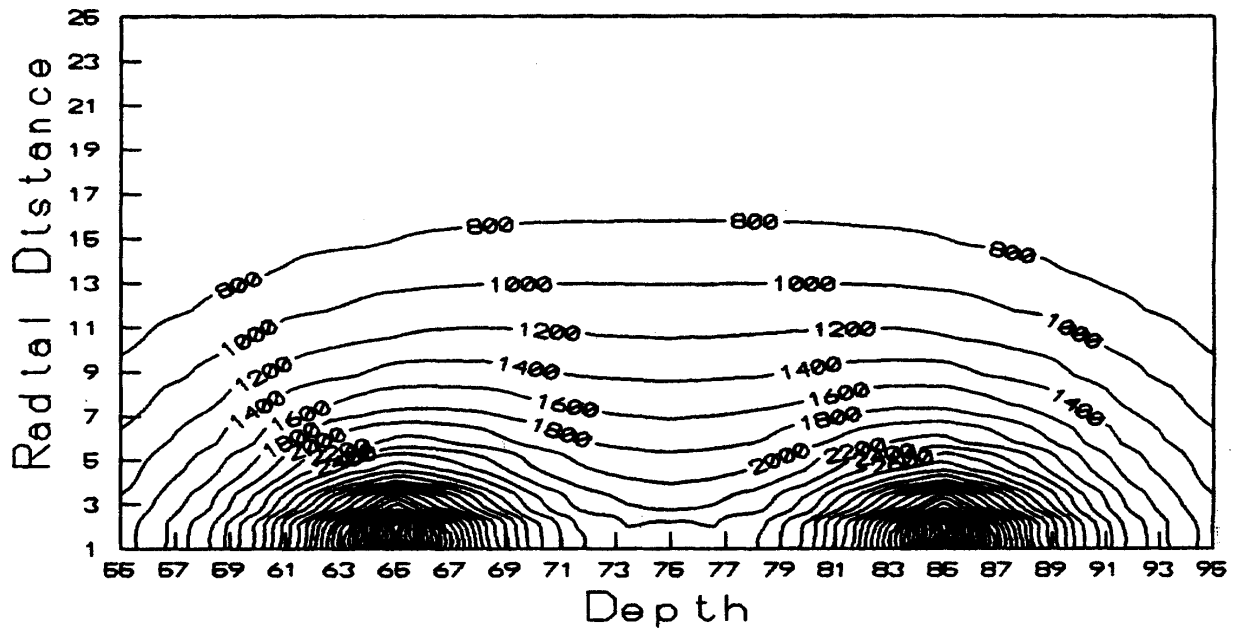


Figure 5. b) Equipotential contour plot in a vertical section for $O_1O_2 = 16''$ and $A_1A_2 = 80''$.

Case II: Bed of Finite thickness ($e/d=50$) with invasion ($D_i=5d$; $R_t/R_m=11$; $R_s = R_m$):

The results of computed normalized apparent resistivity, R_a/R_m versus R_t/R_m along with respective standard values from departure curves (Lynch 1962; N.N, 1958, 1969, 1972) are included in Table 2 and displayed in Fig.4b. In each case, the results were found to be overestimated in comparison with standard results. Further, the degree of overestimation increased with increasing R_t/R_m values primarily due to skipping of low resistivity mud column as explained below.

Case III: Homogeneous bed of infinite thickness with invasion ($R_t/R_m = 11$, $D_i = 5d$):

Standard departure curves (Lynch 1962; N.N, 1958, 1969, 1972) and computed ones are shown in Fig.4c and are included in Table 3. These results tally well with each other.

PERFORMANCE OF LL7 SOFTWARE

Our software, "ll7norm" was next tested for the basic objectives of Laterolog7, i.e., whether focussing is achieved or not, whether a null of potential has actually reached at desired points or not and whether the program is sensitive to changes in current settings or not.

So, an uninvaded bed of infinite thickness having

$R_t/R_m = 100$ was considered. Two different configurations of LL7 as per Table 4 were used to obtain potential values. The relation of current values between auxiliary and main current electrode was chosen as per (Roy 1975) the following relation:

$$\frac{I_0}{I} = \frac{4r^3}{(1-r^2)^2} \quad (7)$$

where $r = O_1O_2/A_1A_2$. In Laterolog 7 (LL7), $r = 0.4$; So, $I_0 = 0.363 I$.

Case I : LL7 with $O_1O_2 = 16''$; $A_1A_2 = 80''$; $O_1O_2 / A_1A_2 = 0.2$;

Main current electrode was placed at grid node number 75 as shown on depth axis of Figs. 5a and 5b.

(i) Potential surface Plot

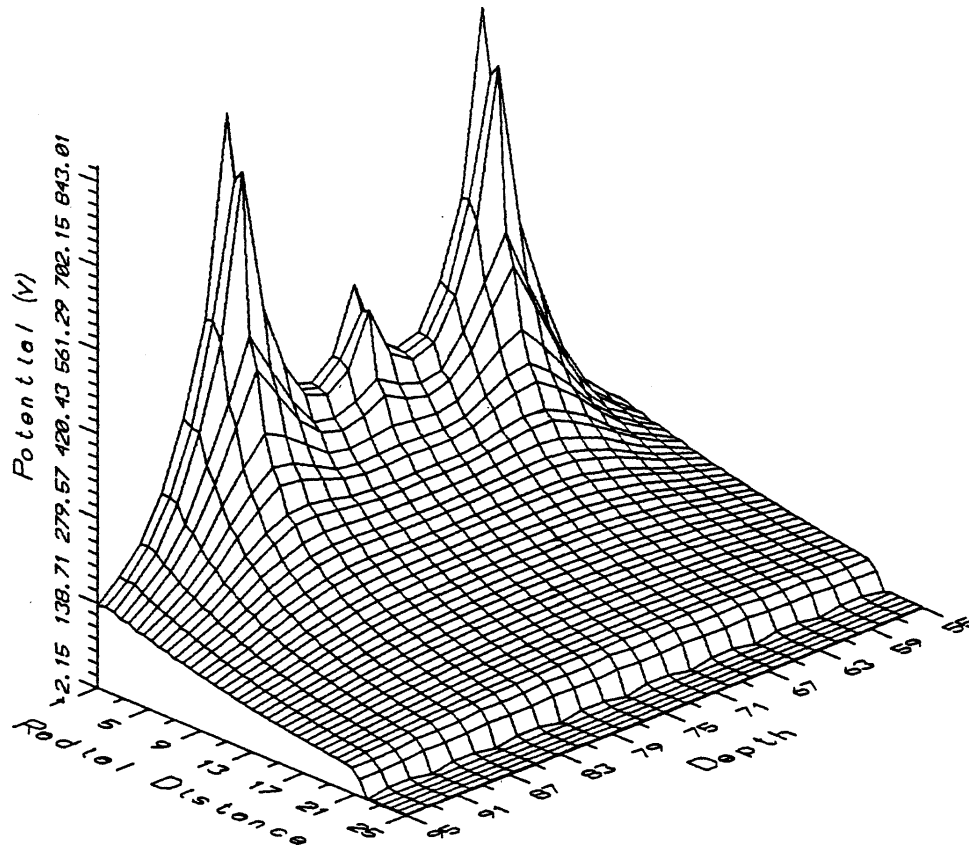
In the potential surface plot (Fig.5a), the depth axis corresponds to bore hole axis along which the tool is run. For clarity sake a front view is shown. Actually, the depth axis would have been behind the plot starting from point of intersection of potential and radial distance axis. The auxiliary electrodes, A_1 and A_2 are at grid nodes 65 and 85 respectively. A potential minima are clearly noticeable at grid nodes 73 and 77, i.e., at $O_1O_2 = 4$ grid units in conformity with theory (Roy 1975).

Table 2. Computed and actual departure curves (R_a/R_m values for different R_t / R_m and AM/d) for Normal device against a finite bed thickness ($e/d = 50.0$) with invasion conditions ($D_i = 2d$; $R_t/R_m = 21$; $R_s = R_m$)

R_t/R_m	R_a/R_m							
	AM/d = 1.5		AM/d = 2.0		AM/d = 4.0		AM/d = 10.0	
	Actual	Computed	Actual	Computed	Actual	Computed	Actual	Computed
21	20.00	22.46	23.33	25.91	28.33	31.22	21.67	25.19
30	26.25	26.25	28.0	33.10	37.50	42.52	32.50	37.50
42	30.0	34.69	36.25	41.54	50.00	56.37	45.00	54.24
70	40.0	47.56	50.0	58.21	70.00	84.89	80.00	93.25
105	55.0	60.77	65.0	75.44	100.00	115.53	125.00	140.28

Table 3. Computed and actual departure curves (R_a/R_m values for different R_t / R_m and AM/d) for Normal device against an infinitely thick bed ($e/d = 50.0$) with invasion conditions ($D_i = 5d$; $R_t/R_m = 11$)

R_t/R_m	R_a/R_m							
	AM/d = 1.5		AM/d = 2.0		AM/d = 4.0		AM/d = 10.0	
	Actual	Computed	Actual	Computed	Actual	Computed	Actual	Computed
22	15.56	18.49	18.89	21.49	28.33	27.50	26.67	26.55
55	25.83	30.19	32.50	36.79	50.00	54.74	65.00	67.85
231	60.00	67.27	80.00	85.78	144.44	147.44	258.33	246.04



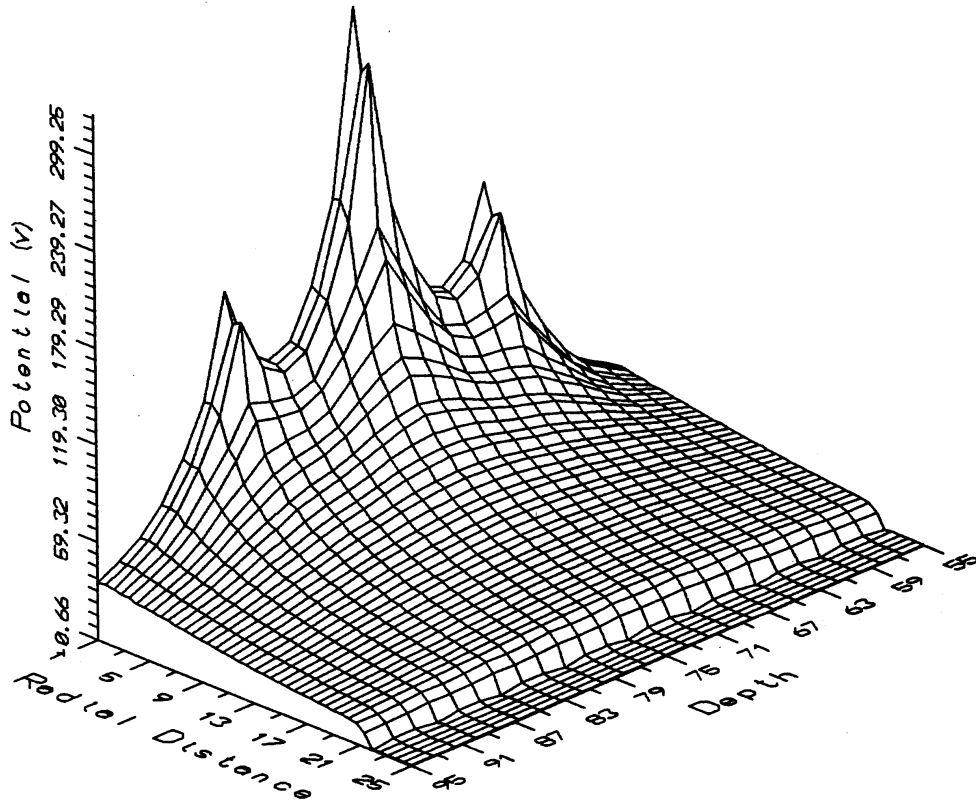


Figure 5. a) Potential surface plot with $O_1O_2 = 48''$ and $A_1A_2 = 80''$.

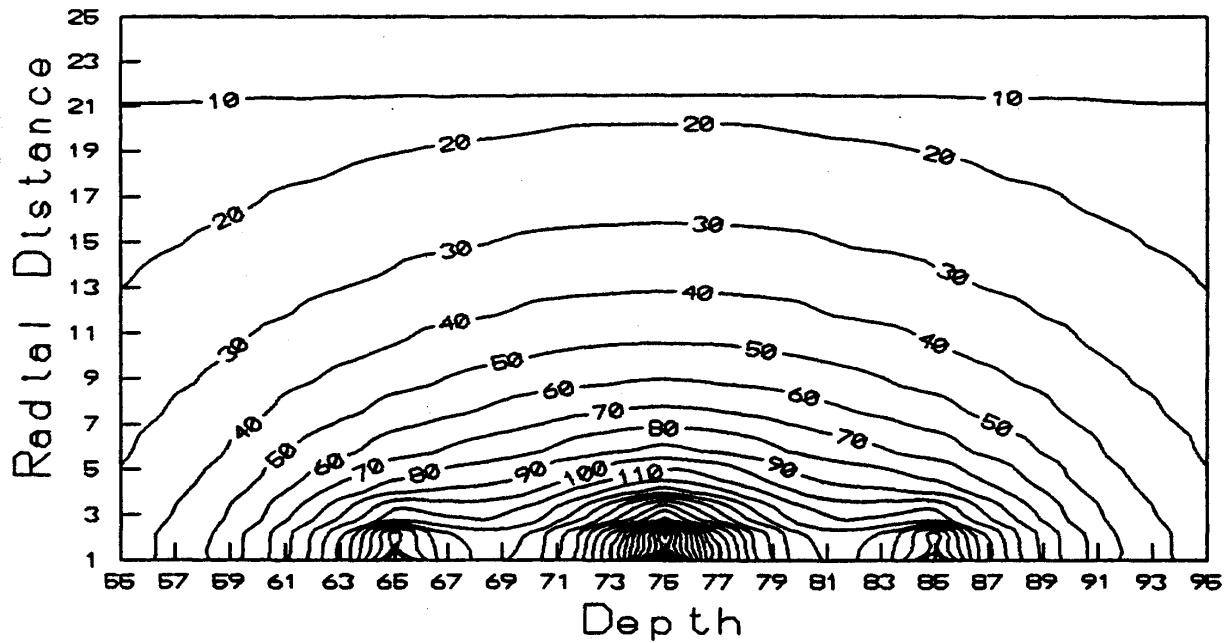


Figure 5. b) Equipotential contour plot in a vertical section for $O_1O_2 = 48''$ and $A_1A_2 = 80''$.

(ii) Equipotential contour plot

Here, in Fig. 5b, near grid node 75 the equipotential contours are nearly parallel to bore hole axis (depth axis), which means that the current lines are orthogonal to these indicating focussing of current into the formation.

Table 4. Variable current settings at auxiliary current electrodes, A_1 and A_2 for a fixed current at main central electrode, A_0 towards ideal current focusing of LL7 device

Distance between two Auxiliary (Guard) electrodes A_1A_2	Distance between null points O_1O_2 in grid units	Current, I_0 from main (central) power electrode, A_0	Current, I from Auxiliary (bucking) power electrodes
20 grid units	2 (8")	100.00	24502.500
= 80"	4 (16")	100.00	2880.500
1 grid unit	8 (32")	100.00	275.625
= 4"	12 (48")	100.00	47.407

Case II $O_1O_2=32"$; $A_1A_2=80"$; $O_1O_2 / A_1A_2 = 0.4$;

(i) Potential Surface plot

Three prominent peaks in potential values are noticeable in Fig.6a corresponding to Current electrode positions, A_0 , A_1 and A_2 with potential minima at grid units 79 and 71 i.e., $O_1O_2 = 8$ unit ($8 \times 4 = 32$ "). Thus the null in potential are reached at desired points.

(i) Equipotential Contour Plot

The equipotential contour plot (Fig.6b) indicates that contour pattern between grid nodes 71 to 79 is parallel to bore hole axis (depth axis), thereby indicating that current lines are orthogonal to these and LL7 device exhibits perfect focussing.

Case III $A_1A_2=80"$, $O_1O_2=48"$; $O_1O_2 / A_1A_2 = 0.6$;

(i) *Potential surface plot* (Fig. 7a) indicates that null is reached at desired points 69 and 81 on grid axis, i.e., $O_1O_2 = 81-69 = 12$ grid units = 48".

(ii) *Equipotential contour plot* shows perfect focussing (Fig.7b).

Thus, in each case focussing was obtained and the software was found to be sensitive to changes in auxiliary current and it can be concluded that Roy's (1975) condition for current focussing of LL7 for infinite, uninvaded homogeneous beds condition (eqn. 7) is correct.

At this stage, to check Roy's (1975) apparent resistivity expression for LL7, a laterolog was computed with standard LL7 configuration ($O_1O_2=32"$, $A_1A_2=80"$) for an uninvaded bed of infinite thickness ($e/d = 50$) with $R_t/R_m = 100$ and $d = 8$ ". The computed log as per Roy's (1975) Laterolog 7 apparent resistivity expression (eqn. 2) and that of Moran's (1976) are shown Fig.8. Moran's (1976) formula (eqn. 5) using a geometric factor of 1.41 seems to fare badly in comparison to that of Roy's (1975), while the results of later are closer to actual R_t/R_m .

NUMERICAL EXPERIMENTS AND RESULTS

After the customary validation of our laterolog software, "ll7norm", the performance of LL7 device with respect to normal device is checked for both constant and variable current ratios.

Case I: Constant Current ratio, $I_0/I (= 0.363)$ as per Roy's (1975)

Beds of various thicknesses were chosen and R_t/R_m was varied from 100 to 800. Both Normal and LL7 logs as per different geometric factors were computed. Here, spacing of Normal log, AM is chosen to be equal to A_1A_2 of laterolog 7. The resulting R_a/R_m plots for different e/d are included in Figs. 9a, 10a, 11a, 12a and 13a. For each of them, relative error, δ (in %) plots are included in Figs. 9b, 10b, 11b, 12b and 13b with the following definition for relative error (in %):

$$\epsilon\% = \frac{(R_t / R_m - R_a / R_m)}{R_t / R_m} 100 \tag{7}$$

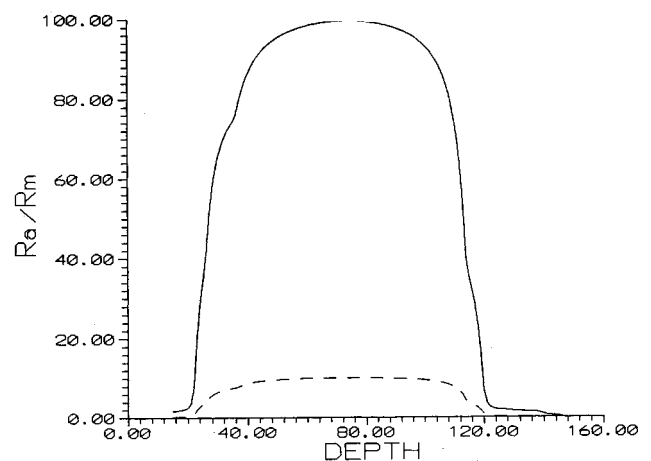


Figure 8. LL7 ($A_1A_2 = 80"$ and $O_1O_2 = 32"$) responses (R_a/R_m versus Depth for $R_t/R_m = 100$) using Roy's (1975) and Moran's (1976) apparent resistivity formulae against a thick bed with no invasion

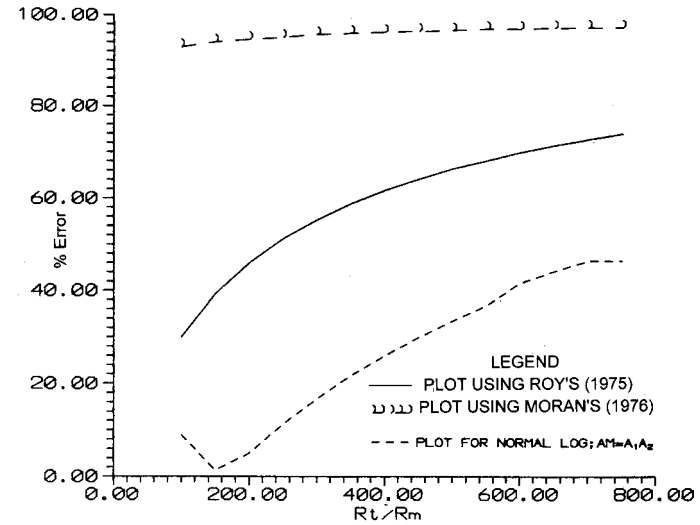
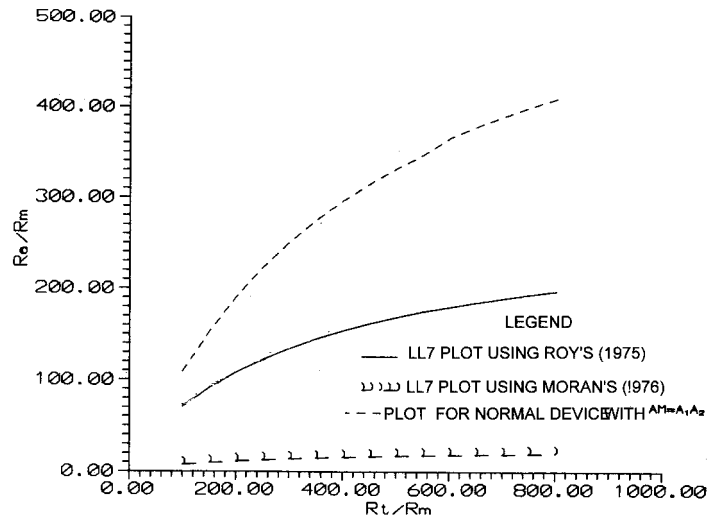


Figure 9. a) Comparison of LL7 plots (R_a/R_m versus R_t/R_m) for different geometric factors and equivalent Normal logs ($AM = A_1A_2$) against a finite - thickness invaded bed ($D_i=5d$; $R_i/R_m = 11$; $e/d = 50$; $d = 2$; $R_s/R_m = 1$) with current setting ($I_0/I = 0.363$) as per Roy (1975). b) Relative error plot (%) for R_a/R_m versus R_t/R_m for different geometric factors of LL7 with rest of conditions as per above (Fig. 9a)

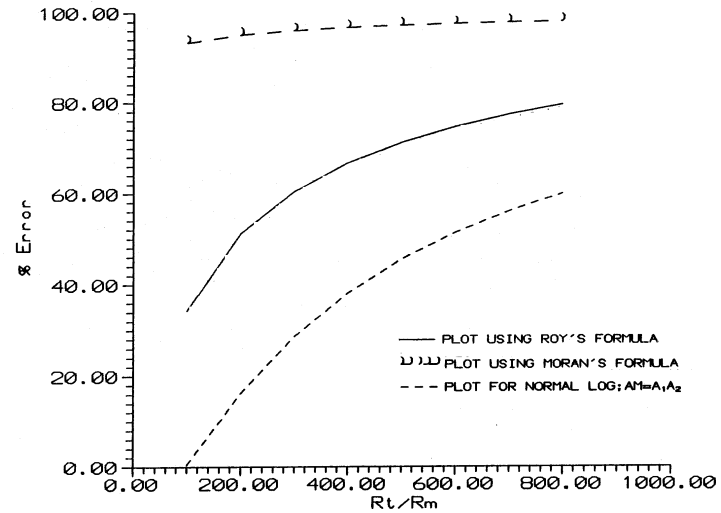
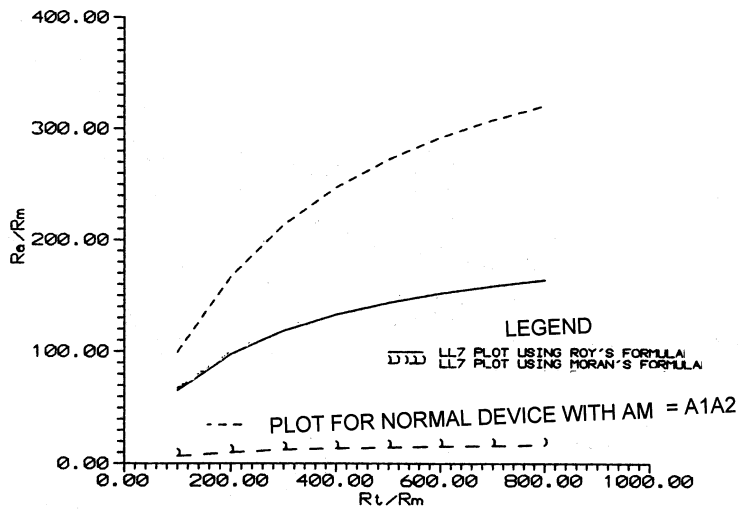


Figure 10. a) Comparison of LL7 plots (R_a/R_m versus R_t/R_m) for different geometric factors and equivalent Normal logs ($AM = A_1A_2$) against a finite - thickness invaded bed ($D_i=5d$; $R_i/R_m = 11$; $e/d = 40$; $d = 2$; $R_s/R_m = 1$) with current setting ($I_0/I = 0.363$) as per Roy (1975). b) Relative error plot (%) for R_a/R_m versus R_t/R_m for different geometric factors of LL7 with rest of conditions as per above (Fig. 10a)

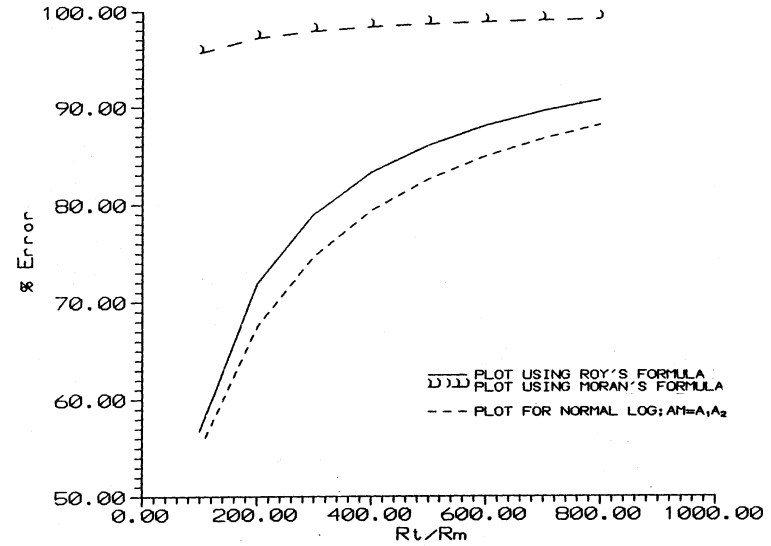
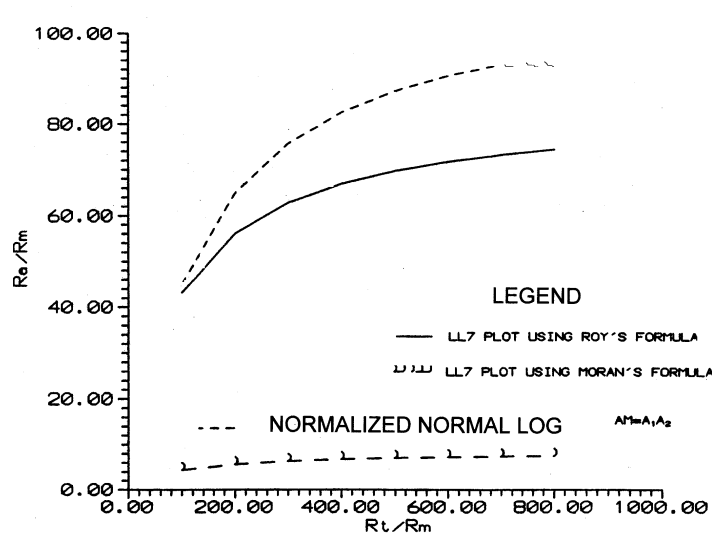


Figure 11. a) Comparison of LL7 plots (R_a/R_m versus R_i/R_m) for different geometric factors and equivalent Normal logs ($AM = A_1A_2$) against a finite - thickness invaded bed ($D_i = 5d$; $R_i/R_m = 11$; $e/d = 20$; $d = 2$; $R_s/R_m = 1$) with current setting ($I_0/I = 0.363$) as per Roy (1975). b) Relative error plot (%) for R_a/R_m versus R_i/R_m for different geometric factors of LL7 with rest of conditions as per above (Fig. 11a)

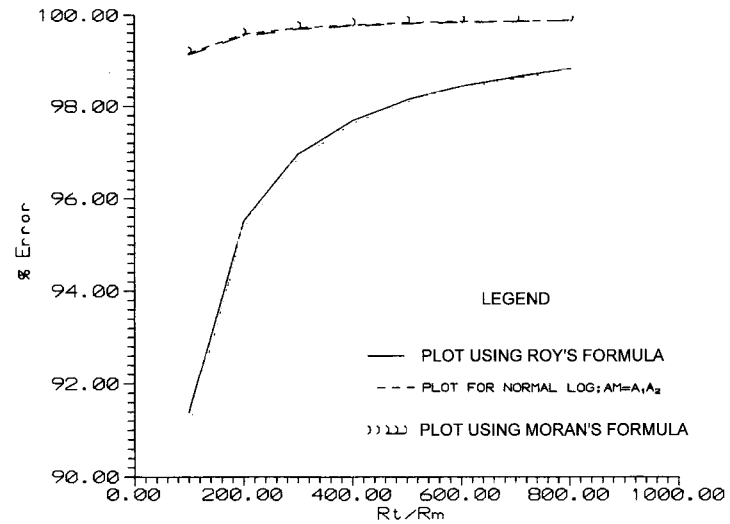
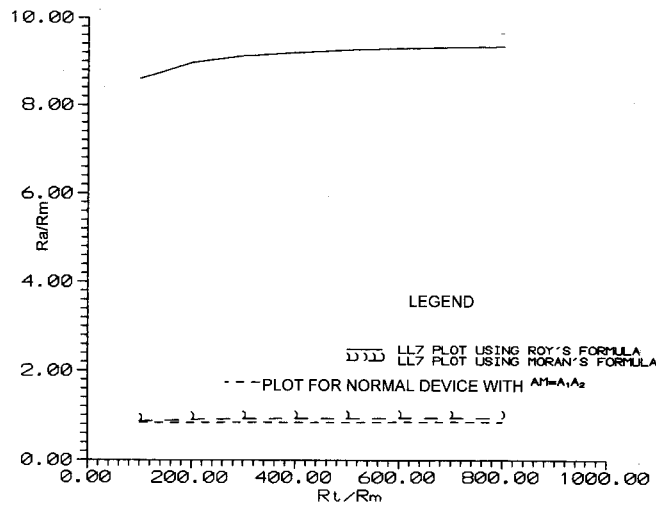


Figure 12. a) Comparison of LL7 plots (R_a/R_m versus R_i/R_m) for different geometric factors and equivalent Normal logs ($AM = A_1A_2$) against a finite - thickness invaded bed ($D_i = 5d$; $R_i/R_m = 11$; $e/d = 10$; $d = 2$; $R_s/R_m = 1$) with current setting ($I_0/I = 0.363$) as per Roy (1975). b) Relative error plot (%) for R_a/R_m versus R_i/R_m for different geometric factors of LL7 with rest of conditions as per above (Fig. 12a)

The following points emerge from Figs 9 – 13:

a) The Laterolog response with Moran's (1976) Geometric Factor: The computed R_a/R_m as per Moran's formula (eqn.5) drastically deviates from actual R_t/R_m and relative error (ϵ %) is always greater than 90. This behavior is primarily due to fixed current setting, I_0/I and it does not conform to the real practice of LL7 (Moran 1976).

b) The Laterolog response with Roy's (1975) Geometric Factor: For relatively thick beds ($e/d = 50$) and low R_t/R_m , the estimated R_a/R_m is reasonable with relative error, ϵ % well within 30%. For e/d of 40, the relative error for computed R_a/R_m , ϵ % > 60% for $R_t/R_m = 350$. For $e/d = 10$, ϵ % > 90% even for low $R_t/R_m = 200$. For $e/d < 1$, i.e., less than A_1A_2 spacing, the Normal tool crashed and the results are more than 95% in error. This amount of error even exhibited when bed thickness, $e > O_1O_2$. For $e/d = 2$, the Normal device became insensitive to changing R_t/R_m . Thus, the advantages resulting from focusing became illusory (Roy 1975).

c) The equivalent Normal response with $AM = A_1A_2$: The general behavior of Normal log was found to be better than all LL7 responses for beds of moderate bed thickness. However, with decreasing bed thickness, the difference between Normal and Laterolog 7 responses got reduced, for e.g., $e/d = 20$ and the relative error in R_a/R_m increased beyond 50%. The Normal log failed for $e/d = 10$, i.e., $e = AM$, and as per theoretical predictions shown the resistive beds

Table 5. Formation parameter combinations (as dimensionless ratios) that are utilized in numerical experiments for current setting of LL7 as per Roy (1975)

$d = 8''$ (2 grid units); $R_t/R_m = 11$; $D_i = 5d$; $I_0/I = 0.363$; $R_s/R_m = 1$;			
Current Ratio used	R_t/R_m	e/d	$e/A_1A_2 = e/AM$
Roy (1975)	100 – 800 with an interval of 100	50,40,30, 20,10,5,2	5,4,3,2, 1,0.5,0.2

to be conductive even (Lynch 1962). Further, the relative error for normal device rises with increasing R_t/R_m and decreasing e/AM .

So far, the results were obtained with fixed current ratio, which as per Moran (1976) is violation of Laterolog 7 principles of operation, as null potential is not obtained at desired points 71 and 79 grid nodes on depth axis except for $e/d = 50$ case.

Hence, the following detailed experiments for variable current settings against inhomogeneous earth medium are undertaken to test the relative performance of several Laterolog 7 devices and Normal device.

Case II: Numerical experiments with Variable Current ratios

Here, conditions for perfect focusing were achieved using variable currents from auxiliary current

Table 6. Range of R_t/R_m for which synthetic R_a/R_m possesses relative error less than 30% answering different e/d values under fixed (Roy, 1975) and variable current ratios, I_0/I (LL7 device)

Nature of current ratio, I_0/I	Device	$e/d=50$, $e/A_1A_2 = e/AM=5$	$e/d=40$, $e/A_1A_2 = e/AM=4$	$e/d=30$ $e/A_1A_2 = e/AM=3$	$e/d=20$ $e/A_1A_2 = e/AM=2$	$e/d=10$ $e/A_1A_2 = e/AM=1$	$e/d=2$ $e/A_1A_2 = e/AM=0.2$
Constant $I_0/I=0.363$ (Roy, 1975)	Normal ($AM=A_1A_2$)	100-500	100-320	100-160			
	LL7 Geometric Factor as per Roy(1975)	£ 100					
	LL7 Geometric Factor as per Moran (1976)						
Variable Current (Praveer, 1997)	LL7 Geometric Factor as per Roy (1975)	£ 100					
	LL7 Geometric Factor as per Moran (1976)						

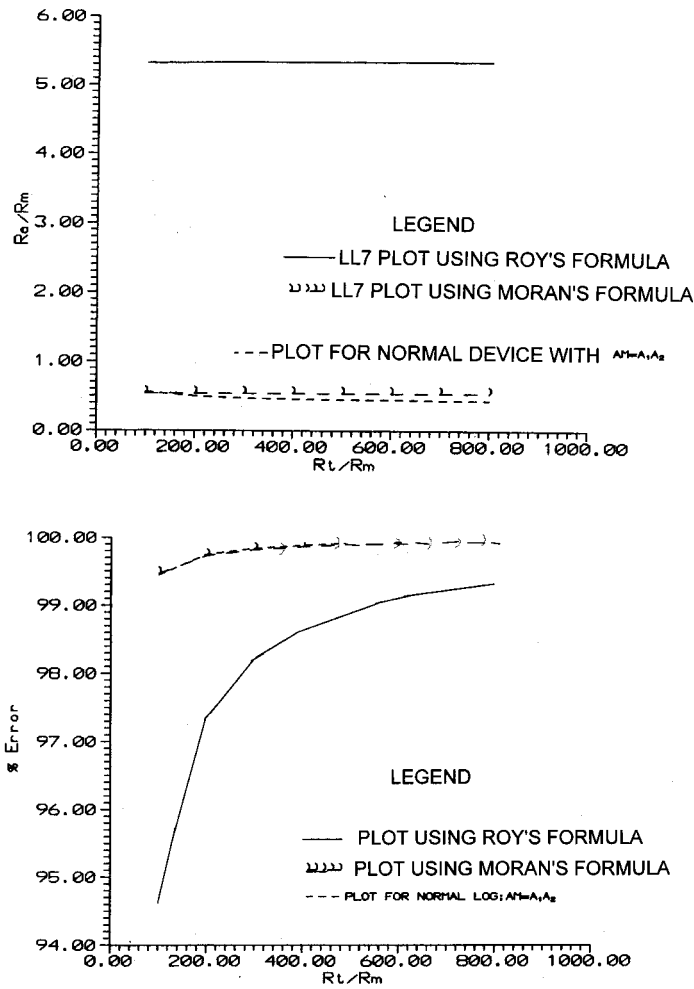


Figure 13. a) Comparison of LL7 plots (R_a/R_m versus R_t/R_m) for different geometric factors and equivalent Normal logs ($AM = A_1A_2$) against a finite - thickness invaded bed ($D_1 = 5d$; $R_t/R_m = 11$; $e/d = 2$; $d = 2$; $R_s/R_m = 1$) with current setting ($I_0/I = 0.363$) as per Roy (1975). b) Relative error plot (%) for R_a/R_m versus R_t/R_m for different geometric factors of LL7 with rest of conditions as per above (Fig. 13a)

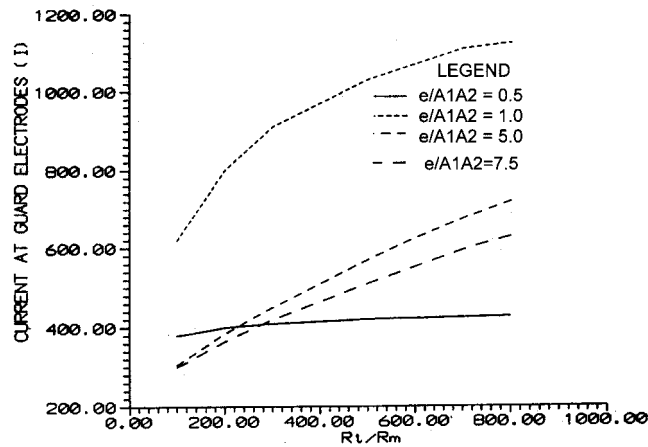


Figure 14. Plot of current settings at guard electrodes as a function of R_t/R_m for different e/A_1A_2 values to achieve perfect focusing in inhomogeneous medium.

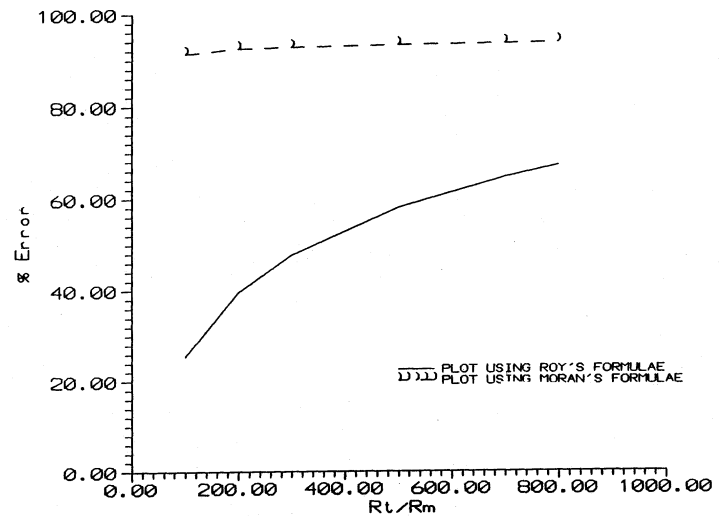
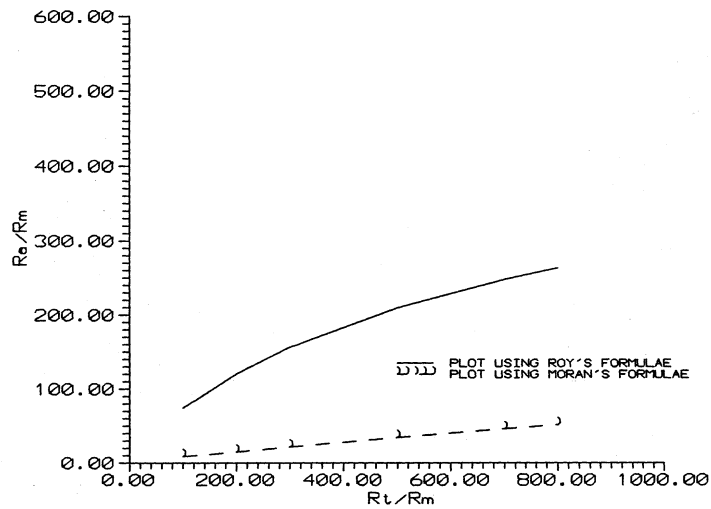


Figure 15. a) Comparison of LL7 responses in terms of R_a/R_m versus R_t/R_m using different geometric factors and variable current settings at guard electrodes under perfect focusing of current at central electrode into resistive medium ($A_1A_2 = 80'' = 20$ grid units; $O_1O_2 = 32'' = 8$ grid units; $R_s/R_m = 1$; $d = 8''$; $D_i = 5d$; $R_t/R_m = 11$; $e/A_1A_2 = 7.5$; $e/d = 75$). b) Plot of relative error (%) in estimation of R_a/R_m for different R_t/R_m using different geometric factors for LL7 device with rest of conditions as per Fig. 15 a.

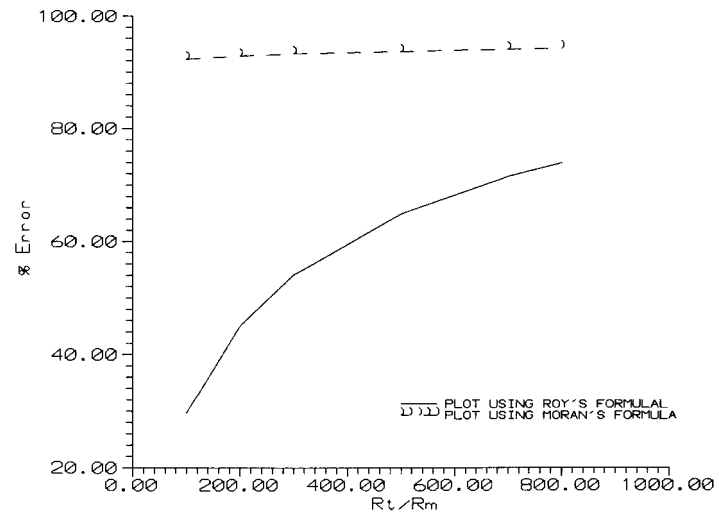
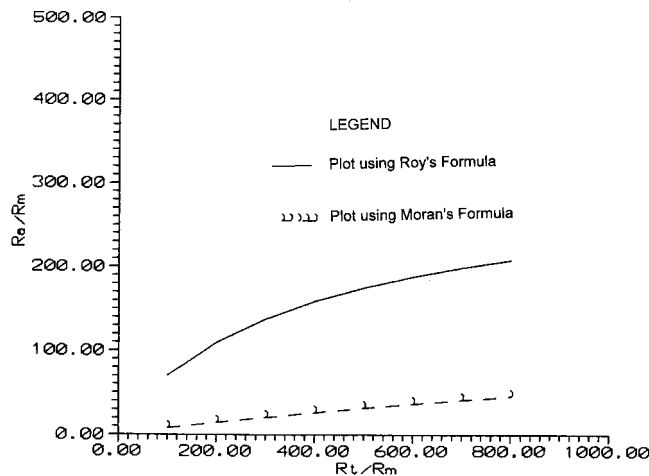


Figure 16. a) Comparison of LL7 responses in terms of R_a/R_m versus R_t/R_m using different geometric factors and variable current settings at guard electrodes under perfect focusing of current at central electrode into resistive medium ($A_1A_2 = 80'' = 20$ grid units; $O_1O_2 = 32'' = 8$ grid units; $R_s/R_m = 1$; $d = 8''$; $D_i = 5d$; $R_t/R_m = 11$; $e/A_1A_2 = 5$; $e/d = 50$). b) Plot of relative error (%) in estimation of R_a/R_m for different R_t/R_m using different geometric factors for LL7 device with rest of conditions as per Fig. 16 a.

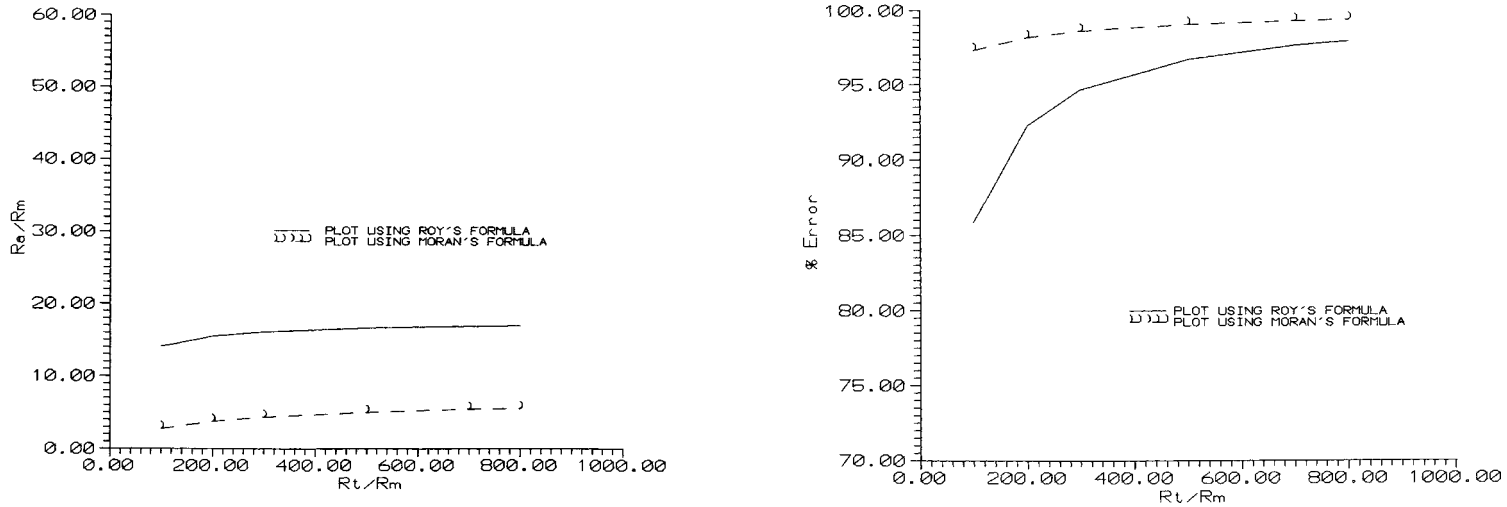


Figure 17. a) Comparison of LL7 responses in terms of R_a/R_m versus R_t/R_m using different geometric factors and variable current settings at guard electrodes under perfect focusing of current at central electrode into resistive medium ($A_1A_2 = 80'' = 20$ grid units; $O_1O_2 = 32'' = 8$ grid units; $R_s/R_m = 1$; $d = 8''$; $D_i = 5d$; $R_i/R_m = 11$; $e/A_1A_2 = 1$; $e/d = 10$). b) Plot of relative error (%) in estimation of R_a/R_m for different R_t/R_m using different geometric factors for LL7 device with rest of conditions as per Fig. 17 a.

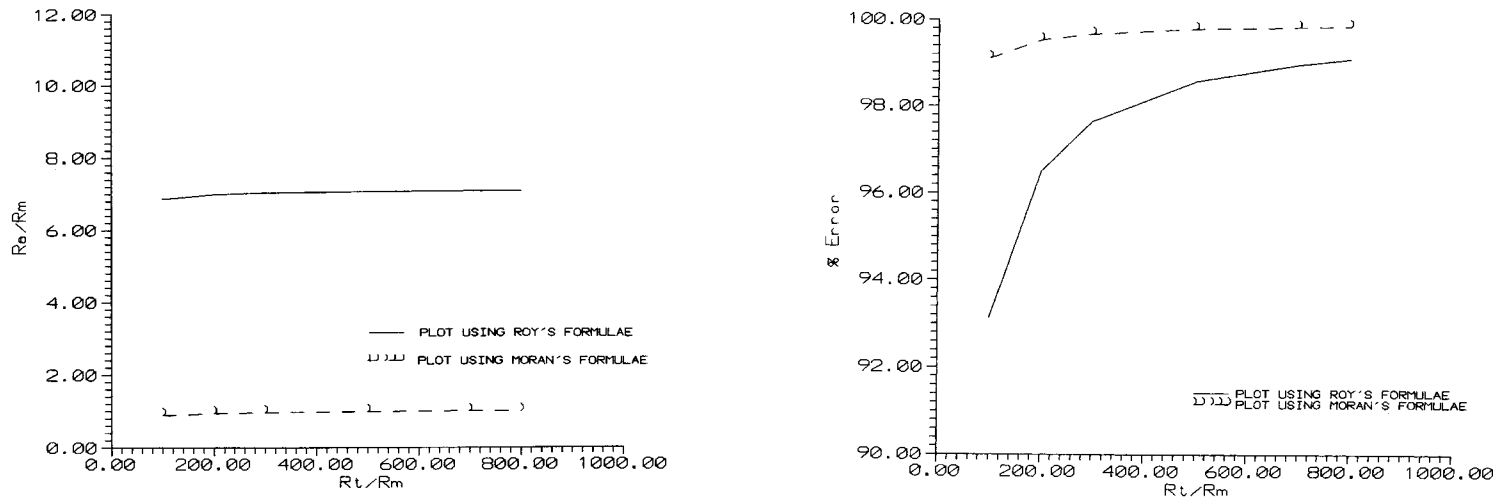


Figure 18. a) Comparison of LL7 responses in terms of R_a/R_m versus R_t/R_m using different geometric factors and variable current settings at guard electrodes under perfect focusing of current at central electrode into resistive medium ($A_1A_2 = 80'' = 20$ grid units; $O_1O_2 = 32'' = 8$ grid units; $R_s/R_m = 1$; $d = 8''$; $D_i = 5d$; $R_i/R_m = 11$; $e/A_1A_2 = 0.5$; $e/d = 5$). b) Plot of relative error (%) in estimation of R_a/R_m for different R_t/R_m using different geometric factors for LL7 device with rest of conditions as per Fig. 18 a.

electrodes (Ref. Table 5). The magnitude of auxiliary (bucking) current required for perfect focusing answering different values of R_t/R_m and e/A_1A_2 is shown in Fig. 14. The achieved results (R_a/R_m and its relative error computation) are included in Fig. 15 – 18. Contrary to expectation, Moran's (1976) LL7 log did not improve and its dismal performance continued in contrast to Roy's (1975).

The Normal device, spacing for spacing (with $AM=A_1A_2$), was however better for low R_t/R_m (<500). For $R_t/R_m > 500$, performance of LL7 device is comparatively better than a Normal device.

For thin beds of $e/d = 10$, the relative error in R_a/R_m was always greater than 70%. With $e/d = 5$, this error was greater than 90% for all R_t/R_m values. The ranges of R_t/R_m estimation well within 30% error limit are included in Table 5 for all studied devices.

Thus, Table 6 summarizes the relative performance of these devices. The blank entries in Table 6 stress the point that the error in R_a/R_m to that of R_t/R_m far exceeds the set arbitrary error limit of 30%.

DISCUSSION

The overestimation in computed R_a/R_m in case of invaded finite thickness bed at validation stage is primarily due to insufficient conductivity assignment for the borehole mud, flushed and invaded zones. This situation arose because of chosen FDM grid size to be 4". Referred to Fig. 2b, $j = 1$ to $j = 2$ is bore hole extent. This region is supposedly filled with mud. There is no element/node, where values of R_{x_0} can be assigned. At $j = 3$, average of R_{x_0} and R_1 is assigned. Thus, a low resistive column is skipped in the model. The remedy lies in increasing diameter of invasion, which is implemented in outlined Case III.

The phrase "spacing for spacing" used along with computed Normal log refers to Normal device (Roy 1975) equivalent in effective spacing $AM = A_1A_2$ of LL7. The assertion by Roy (1975) that Normal device is indeed a better tool than that of LL7 is valid. Our numerical experiments have placed the bounds for this assertion. In a limited way, our results confirm that there is no satisfactory geometric factor for LL7, which can deal with inhomogeneous medium. This even applies to Roy's (1975) variable geometric factor described by eqn. 3. Our results support the ideas of Roy (1975) in denying the superiority of laterolog devices including LL7 over unfocussed Normal device.

CONCLUSIONS

1. Spacing for spacing, a normal log is better than LL7 as long as $e/AM > 1$ and $R_t/R_m < 500$ for $R_s = R_m$.

2. For LL7 apparent resistivity computation Moran's (1976) formula fared very badly in comparison to Roy's (1975) formulae using both fixed and variable current ratios at main and auxiliary current electrodes of LL7. Roy's (1975) LL7 formula for fixed current ratio is strictly valid for homogeneous medium only and for inhomogeneous medium with $R_t/R_m < 100$, $e/A_1A_2 < 5$ it exhibits a reasonable performance (error $< 30\%$).

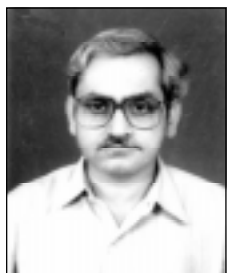
3. Our numerical experiments suggest that separation of auxiliary current electrodes, A_1A_2 is more crucial and the factor $e/A_1A_2 < 1$ affects the performance of both LL7 and equivalent Normal devices. Thus, logging of thin beds of size O_1O_2 spacing (Fig. 2a) by LL7 remains an unrealizable dream.

REFERENCES

- Doll, H.G., 1951. The Laterolog: A new resistivity logging method with electrodes using an automatic focussing system, J. Petrol. Technol., 192, 305-316.
- Doll, H.G., 1953. The microlaterolog, Pet. Trans. AIME, 198, 17-32.
- Drahos, D., 1984. Electrical modeling of the inhomogeneous invaded zone, Geophysics, 49, 1580-1585.
- Guyod, H., 1964. Factors affecting the responses of laterolog type logging systems (LL3 and LL7), J. Pet. Tech., 16, 211-219.
- Hearst, J.R. & Nelson, P.H., 1985. Well logging for physical properties, McGraw-Hill book co., N.Y.
- Jackson, P.D., 1976. Discussion on New results in resistivity well logging, Geophys. Prosp., 24, 407-408.
- Jackson, P.D., 1981. Focused electrical resistivity arrays: Some theoretical and practical experiments, Geophys. Prosp., 29, 601-626.
- Jiao, D. & Sharma, M.M., 1991. An experimental investigation of the resistivity profile in the flushed zone, The Log Analyst, 33, No.2, 145-154.
- Lynch, E.J., 1962. Formation evaluation, Harper & Row, N.Y, pp.422
- Moran, J.H., 1976. Discussion on "New results in resistivity well logging", Geophys. Prosp., 24, 401-402.
- Moran, J.H. & Chemali, R.E., 1979. More on the laterolog device, Geophys. Prosp., 27, 902-930.
- Mufti, I.R., 1980. Finite-difference evaluation of apparent resistivity curves, Geophys. Prosp., 28, 146-166.
- N.N., 1958. Introduction to Schlumberger well logging, Schlumberger Document No.8,

- Schlumberger well surveying Corporation Ltd., USA
- N.N., 1969. Log interpretation principles, Schlumberger well surveying Corporation Ltd., USA.
- N.N., 1972. Log interpretation principles, Schlumberger Documents, Schlumberger well surveying Corporation Ltd., USA.
- Owen, J.H. & Greer, W.J., 1951. The guard electrode logging system, *Pet. Trans. AIME*, 192, 347-356.
- Pallavi Banerjee., 1996. Finite-difference based modelling software for Laterologs and application, Unpublished M.Tech Dissertation, Deptt. Earth Sci., University of Roorkee, Roorkee.
- Praveer, Kumar, 1997. Numerical modelling of focussed devices, Unpublished M.Tech Dissertation, Deptt. Earth Sci., University of Roorkee, Roorkee.
- Repsold, H., 1977. Comments on "New results in resistivity well logging" by Roy, A., and "Laboratory results in resistivity logging" by Roy, A. & Appa Rao., *Geophys. Prosp.*, 25, 533-559.
- Roy, A. & Apparao, A., 1971. Depth of investigation in direct current methods, *Geophysics*, 36, 943-959.
- Roy, A., 1975. New results in resistivity well logging, *Geophys. Prosp.*, 23, 426-448.
- Roy, A. & Appa Rao, A., 1976. Laboratory results in resistivity logging, *Geophys. Prosp.*, 24, 123-140.
- Roy, A., 1976. Reply to comments by J.H. Moran on "New results in resistivity well logging", *Geophys. Prospecting*, Vol. 24, 403-404.
- Roy, A. & Appa Rao, A., (1978). Reply to comments by H. Repsold (*Geophys. Prosp.*, 25 (1977) on "New results in resistivity well logging and "Laboratory results in resistivity logging" *Geophys. Prosp.*, 26, 481-485.
- Roy, A., 1977. The concept of apparent resistivity in laterolog 7, *Geophys. Prosp.*, 25 (4), 730-737.
- Roy, K.K. & Dutta, D.J., 1993. Analysis of Laterolog tool with variable geometric factor, *The Log Analyst*, 34 (4), 24 -32.
- Roy, K.K. & Dutta, D.J., 1997. Relative performance of focused and unfocused devices in a two-dimensional borehole environment, *J Appl. Geophys.*, 36, 181-194.
- Towle, G.H., Whitman, W. & Kim, Jin-hoo., 1988. Electrical log modeling with a finite difference method, *The Log Analyst*, 29, No. 3, 184-195.

(Accepted 2005 April 3. Received 2004 December 7; in original form 2004 June 9)



Dr. Rambhatla G. Sastry has obtained M.Sc(Tech.) degree in Applied Geophysics from Andhra University in July 1973 and Ph.D. degree in Geophysics from Moscow State University, USSR in April 1980. He has served as CSIR Pool Officer at NGRI during 1980-81 and joined the geophysics faculty of Department of Earth Sciences, University of Roorkee during May 1981. Currently he is serving as Associate Professor in Geophysics at IIT, Roorkee. He was Commonwealth Academic Staff Fellow for the year 1989 at Geophysics Department, University of Edinburgh, Edinburgh (U.K.). His research interests include Exploration Geophysics, Geophysical Inversion and Hydrological Modelling.

ANNEXURE I

The governing equation for flow of steady electric current in a inhomogeneous medium is given by

$$\nabla[\sigma(x, y, z)\nabla V(x, y, z)] + q(x, y, z) = \mathbf{0} \quad (1.1)$$

where

q, current source strength (Am⁻³),

σ, conductivity (S/m) and

V, electric potential (Volts).

By incorporating radial symmetry and adopting cylindrical coordinate system, eqn. (1.1) can be written as

$$\frac{\partial}{\partial r} \left[\sigma(r, z) \frac{\partial V(r, z)}{\partial r} \right] + \frac{\partial}{\partial z} \left[\sigma(r, z) \frac{\partial V(r, z)}{\partial z} \right] + \frac{1}{r} \left[\sigma(r, z) \frac{\partial V(r, z)}{\partial r} \right] + q(r, z) = 0 \quad (1.2)$$

for $\forall r > 0$. Equation (1.2) is used for evaluation of potential field due to a point source located on the axis within the subsurface.

Discretization of the medium

The “mesh centered” grid system is adopted here (Fig. 2) for solving partial differential equation by finite-difference method (FDM). The grid is finely spaced near the current source as this is the region of most rapid fluctuation in potential. Whereas, at points far away from current source, where potential fluctuations are relatively slow, the grids are much coarser. and grid spacings increase exponentially as distance from current source increases. Thus, for FDM, only a small portion ABCD of the semi-infinite medium is considered and is divided into a number of rectangular cells, each of which can be replaced by a point. Location of element of model is given as,

$$r = \sum_{k=2}^i \Delta r(k-1:k); \quad z = \sum_{l=2}^i \Delta z(I-1:I) \quad (1.3)$$

where $\Delta r(k-1:k)$, spacing between columns k-1 and k, $\Delta z(I-1:I)$, spacing between rows I-1 and I, i = 1, air-earth interface (z = 0) and j = j_{max} corresponds to boundary BC & i = i_{max} corresponds to boundary CD.

Boundary conditions

For a set of elements, P(i,j) located (Fig.2) inside the boundary ABCDA, For P(i,j) ∈ G, then the boundary conditions are as follows:

$$\frac{\partial V}{\partial z} = \mathbf{0}, \{P(1, j) : i = 1, j = 1, 2, \dots, j_{\max}\} \quad (1.4)$$

implying no current flow across the air-earth interface.

$$\frac{\partial V}{\partial z} = \mathbf{0}, \{P(i, j) : j = 1, i = 1, 2, \dots, i_{\max}\} \quad (1.5)$$

implying a radial symmetry and

$$V = V \left\{ \begin{array}{l} (i, j) : j = j_{\max}, i = 1, 2, \dots, i_{\max} \\ (i, j) : i = i_{\max}, j = 1, 2, \dots, j_{\max} \end{array} \right. = \mathbf{0} \quad (1.6)$$

Derivation of finite difference equations

Conversion of differential equation (1.2) into a simple algebraic equation is done using Taylor's series. Thus, for any element P(i,j) we can represent a differential term into algebraic expression as follows:

$$\begin{aligned} \frac{\partial}{\partial r} \left(r \frac{\partial V}{\partial r} \right) &= \frac{2}{h_E + h_W} \left[\left\{ \sigma \frac{\partial V}{\partial r} \right\}_{i, j+h_E/2} - \left\{ \sigma \frac{\partial V}{\partial r} \right\}_{i, j-h_W/2} \right] \\ &= \frac{2}{h_E + h_W} \left[\frac{\sigma_{i, j+h_E/2}}{h_E} (V_{i, j+h_E} - V_{i, j}) - \frac{\sigma_{i, j-h_W/2}}{h_W} (V_{i, j} - V_{i, j-h_W}) \right] \end{aligned} \quad (1.7)$$

where $\sigma_{i, j+h_E/2} = (\sigma_{i, j} + \sigma_{i, j+h_E}) / 2$ and

$$\sigma_{i, j-h_W/2} = (\sigma_{i, j} + \sigma_{i, j-h_W}) / 2$$

are conductivities at (i,j+h_E/2) and (i,j-h_W/2) respectively in the grid system. h_E, h_W refer to separations of element from its neighbouring elements in east and west directions respectively (Fig. 2). Thus we an equation for each element as below:

$$\begin{aligned} &\frac{2}{h_E + h_W} \left[\frac{\sigma_{i, j+h_E/2}}{h_E} (V_{i, j+h_E} - V_{i, j}) - \frac{\sigma_{i, j-h_W/2}}{h_W} (V_{i, j} - V_{i, j-h_W}) \right] + \\ &\frac{2}{h_N + h_S} \left[\frac{\sigma_{i, j+h_S/2}}{h_S} (V_{i+h_S, j} - V_{i, j}) - \frac{\sigma_{i-h_N/2, j}}{h_N} (V_{i, j} - V_{i-h_N, j}) \right] + \\ &\frac{\sigma_{i, j}}{r(h_E + h_W)} \left[(V_{i, j+h_E}) (V_{i, j-h_W}) \right] + q_{i, j} = \mathbf{0} \end{aligned} \quad (1.8)$$

where h_N and h_S are distances of element north and south of the element under consideration and r is the radial distance of the element from the borehole axis.

After further simplification, the above equations reduce to

$$\alpha_E(i, j)V_{i, j+h_E} + \alpha_N(i, j)V_{i-h_N, j} + \alpha_W(i, j)V_{i, j-h_W} + \alpha_S(i, j)V_{i+h_S, j} - \alpha_P(i, j)V_{i, j} + \bar{q}(i, j) = \mathbf{0} \quad (1.9)$$

where á's are conductivity coefficients given by the following expressions

$$\alpha_E(i, j) = \sigma_{i, j+h_E/2} \left[\frac{1}{h_E} + \frac{1}{2r} \right] \left[\frac{h_N + h_S}{2} \right] \quad (1.10)$$

$$\alpha_W(i, j) = \sigma_{i, j-h_W/2} \left[\frac{1}{h_W} + \frac{1}{2r} \right] \left[\frac{h_N + h_S}{2} \right] \quad (1.11)$$

$$\alpha_N(i, j) = \sigma_{i-h_N/2, j} \left[\frac{1}{h_N} \right] \left[\frac{h_E + h_W}{2} \right] \quad (1.12)$$

$$\alpha_S(i, j) = \sigma_{i+h_S/2, j} \left[\frac{1}{h_S} \right] \left[\frac{h_E + h_W}{2} \right] \quad (1.13)$$

$$\alpha_P(i, j) = \alpha_E(i, j) + \alpha_N(i, j) + \alpha_W(i, j) + \alpha_S(i, j) \quad (1.14)$$

$$\bar{q}(i, j) = q_{i, j} \left[\frac{h_E + h_W}{2} \right] \left[\frac{h_N + h_S}{2} \right] \quad (1.15)$$

Coefficient set for elements lying at origin, on air-earth interface (i = 1) and along borehole axis (j = 1) are computed separately incorporating special conditions (boundary conditions where appropriate) leading to the following:

a) On air-earth interface (i = 1)

$$\alpha_E(1, j) = \sigma_{i, j+h_E/2} \left[\frac{1}{h_E} + \frac{1}{2r} \right] h_S \quad (1.16)$$

$$\alpha_W(1, j) = \sigma_{i, j-h_W/2} \left[\frac{1}{h_W} + \frac{1}{2r} \right] h_S \quad (1.17)$$

$$\alpha_N(1, j) = 0 \quad (1.18)$$

$$\alpha_S(1, j) = 2\sigma_{i+h_S/2, j} \left[\frac{1}{h_S} \right] \left[\frac{h_E + h_W}{2} \right] \quad (1.19)$$

$$\bar{q}(i, j) = q_{i, j} \left[\frac{h_E + h_W}{2} \right] h_S \quad (1.20)$$

b) Along borehole axis (j = 1)

$$\alpha_E(i, 1) = 4\sigma_{i, j} \left[\frac{1}{h_E} \right] \left[\frac{h_N + h_S}{2} \right] \quad (1.21)$$

$$\alpha_W(i, 1) = 0 \quad (1.22)$$

$$\alpha_N(i, 1) = \sigma_{i-h_N/2, 1} \left[\frac{h_E}{h_N} \right] \quad (1.23)$$

$$\alpha_S(i, 1) = \sigma_{i+h_S/2, 1} \left[\frac{h_E}{h_S} \right] \quad (1.24)$$

$$\bar{q}(i, j) = q_{i, j} h_E \left[\frac{h_N + h_S}{2} \right] \quad (1.25)$$

c) At the origin (i=1, j=1)

$$\alpha_E(1, 1) = 8\sigma_{1, 1} \left[\frac{1}{h_E} \right] \left[\frac{h_S}{2} \right] \quad (1.26)$$

$$\alpha_W(1, 1) = 0 \quad (1.27)$$

$$\alpha_N(1, 1) = 0 \quad (1.28)$$

$$\alpha_S(1, 1) = 2\sigma_{i+h_S/2, 1} \left[\frac{h_E}{h_S} \right] \quad (1.29)$$

$$\bar{q}(i, j) = q_{1, 1} h_E h_S \quad (1.30)$$

The difference equations (1.9) are solved by considering the boundary conditions (Eqns. 1.10 –1.30) through an efficient solver such as successive over relaxation method (SOR).